Journal of Engineering Mathematics 23: 283–293, 1989

The cubic autocatalator: the influence of degenerate singularities in a closed system

B.F. GRAY and R.A. THURAISINGHAM
School of Chemistry, Macquarie University, Sydney, N.S.W. 2109, Australia

Received 6 December 1988; accepted 20 February 1989

Abstract. The appearance of apparently chaotic behaviour in this two-dimensional system is examined from an analytical point of view. The original two-parameter model exhibiting numerical solutions resembling chaos is unfolded to a three-parameter model. This enlarged model is shown to have a codimension-two degenerate Hopf bifurcation the unfolding of which contains phase portraits showing three concentric limit cycles.

In some regions these limit cycles are so close to each other that numerical integration causes transitions across the unstable limit cycle, giving the appearance of chaotic behaviour. The region in parameter space of the 'chaotic' behaviour agrees well with the degenerate behaviour of the enlarged model.

1. Introduction

The cubic autocatalator is a model reaction scheme which is very simple but at the same time shows rather exotic behaviour, i.e. highly nonlinear periodic behaviour. It was originally introduced by Gray and Scott [1] and has been discussed in various contexts by a number of authors, e.g. Gray and Scott [2], D'Anna et al. [3], and Merkin, Needham and Scott [4] and Gray, Roberts and Merkin [5]. In [4] and [5] the scheme has been used to model reactions in a closed system (i.e. closed to matter transfer), where the 'pool chemical approximation' is made [4].

In this case the chemical kinetic scheme is

$$\begin{aligned} &\mathrm{P} \quad \rightarrow \mathrm{A}, \quad \text{rate } k_0 P, \\ &\mathrm{A} + 2\mathrm{B} \rightarrow 3\mathrm{B}, \quad \text{rate } k_1 ab^2, \\ &\mathrm{B} \quad \rightarrow \mathrm{C}, \quad \text{rate } k_2 b, \end{aligned}$$

where P, the original reactant, is present in large excess and hence its concentration can be taken to be constant in time (at its initial value) throughout the period of time with which we are concerned.

The differential equations describing this scheme are

$$\mathrm{d}x/\mathrm{d}t = \mu - xy^2, \tag{1}$$

$$\mathrm{d}y/\mathrm{d}t = xy^2 - y, \tag{2}$$

where $x = (k_1/k_2)^{1/2}a$, $y = (k_1/k_2)^{1/2}b$ are the dimensionless concentrations of A and B respectively, $t = k_2 t$ is dimensionless time (t = time) and $\mu = (k_1/k_2)^{1/2}k_0 P_0/k_2$ is a dimensionless rate constant.

Merkin, Needham and Scott [4] analysed equations (1), (2), showing in particular the

bifurcation of a stable limit cycle at $\mu = 1$ and the consequent divergence of the amplitude of this limit cycle in the phase plane at $\mu = 0.9003$. They also studied the effect of the inclusion of the uncatalysed reaction

$$A \rightarrow B\,, \quad \text{rate } k_3 a\,,$$

described by the differential equations

$$dx/dt = \mu - xy^2 - rx\,, \tag{3}$$

$$dy/dt = xy^2 - y + rx\,, \tag{4}$$

where $r = k_3/k_2$. They showed that the system (3), (4) exhibited two Hopf bifurcations, both to stable limit cycles at values of μ which tend to either 1 or 0 as $r \rightarrow 0^+$. The amplitude of the limit cycle is finite over the whole range of μ for which it exists. This range tends to zero as $r \rightarrow 1/8$ at which point a 'double Hopf' or $H2_1$, bifurcation occurs (see Gray and Roberts [6] for an explanation of this notation).

For sufficiently small values of r, the bifurcation diagram for the system (3), (4) is shown in Fig. 1. Although no divergence of amplitude occurs near $\mu = 0.9003$ there appears to be *extreme* sensitivity of both the amplitude and frequency of the oscillation to variation of μ. The purpose of the present paper is to investigate this phenomenon of a 'canard' [7] by unfolding the model (3), (4) further by addition of an extra reaction, which can then be

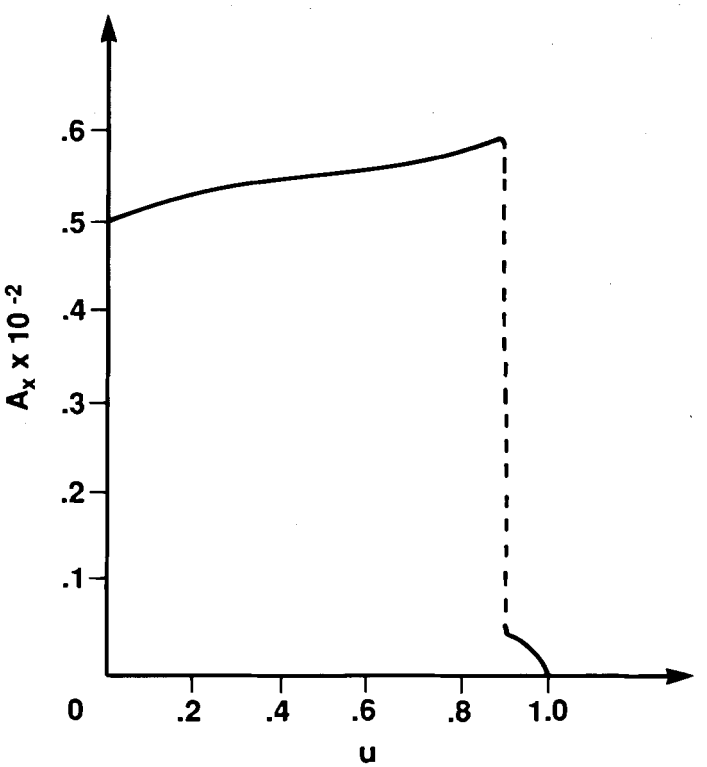

Fig. 1. Variation of amplitude A_x as a function of μ, $r = 10^{-4}$.

allowed to tend to zero. As we shall see this procedure indicates that the 'canard' is in fact a genuine discontinuity and that the model (3), (4) shows behaviour characteristic of a non-universally unfolded system.

This particular point can be seen more clearly if we do not make the 'pool chemical approximation', and in fact allow P to be consumed very slowly. The concentration of P is not coupled to x and y, and it is simply an exponentially decaying function of time. In equations (1), (2), it is replaced by a slowly decreasing function of time:

$$dx/dt = \mu\, e^{-\varepsilon t} - xy^2 - rx\,, \tag{5}$$

$$dy/dt = xy^2 - y + rx\,, \tag{6}$$

where $\varepsilon = k_0/k_2$ (see [4]). For sufficiently small ε, numerical integration of these equations is akin to plotting a 'quasi-static' bifurcation diagram with μ as the (very slowly varying) bifurcation parameter.

The results are shown in Fig. 2 for $r = 10^{-5}$ and $\varepsilon = 10^{-8}$. In Fig. 2a we initially have the

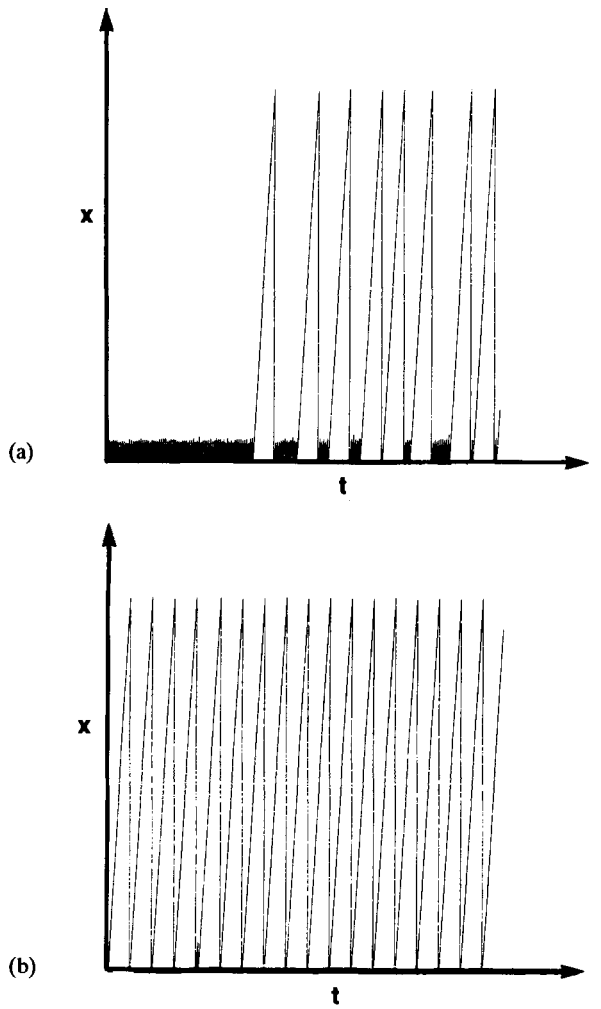

Fig. 2. Amplitude of oscillation A_x as a function of time, $r = 10^{-5}$, $\varepsilon = 10^{-8}$. (a) $\mu = 0.90032$. (b) $\mu = 0.90023$.

'Hopf oscillations', fitting reasonably to the Hopf amplitude formula. The origin corresponds to $\mu = 0.90032$. Before $\mu = 0.90028$ is reached, qualitatively different oscillations appear in a 'chaotic' manner. As μ decreases further they gradually displace the small oscillations until at $\mu = 0.90018$ they have taken over completely. The range of μ for which this phenomenon occurs is extremely small and dependent on r. For $r = 10^{-4}$ the two equations (3) and (4) have been integrated numerically for $\mu = 0.899870$. In Fig. 3a the apparently chaotically mixed oscillations are still present. In Fig. 3b the phase portrait for this case throws considerable light on the numerical results. There appear to be two stable limit cycles (and clearly at least one unstable one between) which are *extremely* close together along two very significant segments, i.e. the two axes $x = 0$, $y = 0$, apart from close to the origin. Manipulation of our parameters of numerical integration did not influence our results, nor did use of either Gear or Runge–Kutta techniques.

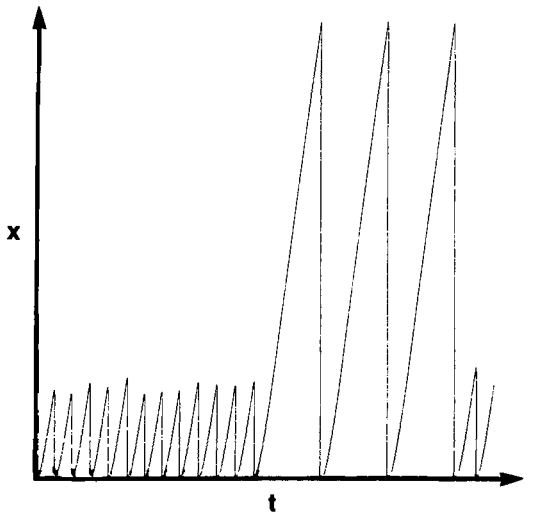

Fig. 3(a). Amplitude of oscillation A_x as a function of time $\mu = 0.899870$, $r = 10^{-4}$.

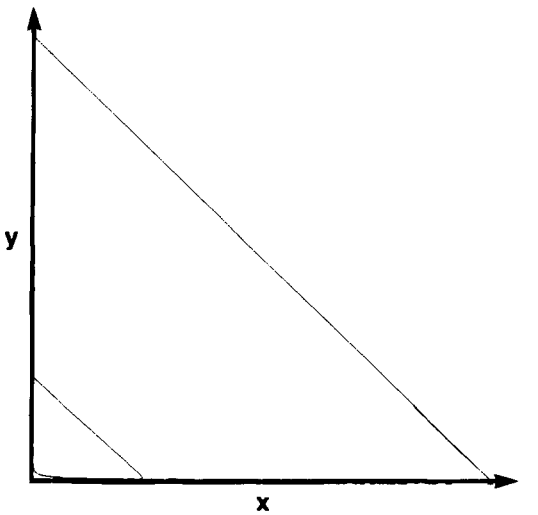

Fig. 3(b). Phase portrait Y *vs.* X for $\mu = 0.899870$, $r = 10^{-4}$.

Certainly the equations in question (3 and 4) cannot exhibit chaotic behaviour although their difference counterparts can and certainly do. In the next section we enlarge the reaction scheme to provide a third parameter which shows the existence of a degenerate singularity containing in its universal unfolding a phase portrait containing three limit cycles surrounding an unstable singularity.

2. The unfolded model

We add to the original reaction scheme a further chemical reaction, the decomposition of A directly to some inert product:

$$A \rightarrow D\,, \quad \text{rate } k_4 a\,,$$

so the generalised differential equations we consider are

$$dx/dt = \mu - xy^2 - (\alpha + r)x\,, \tag{7}$$

$$dy/dt = xy^2 - y + rx\,, \tag{8}$$

where $\alpha = k_4/k_2$. These equations, containing the bifurcation parameter μ and two unfolding parameters α, r, are treated here by the methods outlined in Gray and Roberts [6] which are capable of giving complete qualitative information on the bifurcation diagrams and phase portraits arising from (7), (8). However, this technique needs numerical backup in cases such as the present one. For example, we show that the system (7), (8) must exhibit a phase portrait containing three limit cycles surrounding an unstable singularity, but we cannot show that this region intersects the $\alpha = 0$ axis in parameter space without numerical integration.

The singularities of equations (7) and (8) are defined by

$$\mu - x_s y_s^2 - (\alpha + r)x_s = 0\,, \tag{9}$$

$$x_s y_s^2 - y_s + r x_s = 0\,, \tag{10}$$

and it is clear that there may be up to three solutions of these equations for some parameter values, so an investigation of steady-state bifurcations is necessary in addition to study of the dynamic bifurcations already referred to. The locus of saddle-node bifurcations can be conveniently parametrised by x_s in the form

$$r = \frac{\alpha(\alpha x_s^2 - 1)}{(2\alpha x_s^2 - 1)^2}\,, \tag{11}$$

$$\mu = \frac{2\alpha^2 x_s^3}{(2\alpha x_s^2 - 1)}\,. \tag{12}$$

Since r, μ, $\alpha > 0$ we impose $x_s > 1/\sqrt{\alpha}$. These codimension-zero bifurcations can degenerate to a codimension-one bifurcation of hysteresis type, with defining conditions [6]

$$\frac{dx}{dt} = \frac{dy}{dt} = \frac{d\mu}{dx_s} = \frac{d^2\mu}{dx_s^2} = 0\,, \tag{13}$$

where μ and y_s are regarded as functions of x_s. From (13), some algebra gives us

$$r = \alpha/8 \tag{14}$$

as the locus of the hysteresis bifurcation in the codimension-one (r, α) plane. (N.B. the lower-codimension saddle-node locus is best represented in projection in a codimension-zero plane, either (μ, r) or (μ, α). Alternatively it can be regarded as a surface in (μ, r, α) space, and the hysteresis locus regarded as a curve in this space. We prefer the former interpretation for ease of presentation.) There are no more highly degenerate steady-state bifurcations in this model.

Nondegenerate Hopf bifurcations are defined by equations (9) and (10) together with

$$\operatorname{tr} J = 0\,, \qquad \det J > 0\,, \tag{15}$$

where J is the Jacobian matrix for the system (7) and (8). This bifurcation can also be parametrised by x_s, and for any given $\alpha > 0$ we can write

$$r = \frac{(\alpha+1)[(1-\alpha)x_s^2 - 1]}{(2x_s^2 - 1)^2}\,, \tag{16}$$

$$\mu = \frac{x_s(2\alpha x_s^2 + 1)}{(2x_s^2 - 1)}\,, \tag{17}$$

with the physical restriction $x_s > (1-\alpha)^{-1/2} 1 > \alpha > 0$. Note that the representation (16) and (17) does not take account of the sign of $\det J$.

Degenerate Hopf bifurcations of codimension one are of two types, $H2_1$ and $H3_1$. The $H2_1$ type is defined by equations (9), (10), (15) and

$$\frac{\mathrm{d}}{\mathrm{d}\mu}(\operatorname{tr} J) = 0\,. \tag{18}$$

These conditions can be reduced explicitly, after a little algebra, to

$$r = \frac{(1-\alpha)^2}{8} \quad (\det J > 0)\,. \tag{19}$$

For $H3_1$-type degenerate Hopf bifurcations (where the limit cycle concerned changes stability) equation (18) is replaced by the condition

$$Ax_s^6 + Bx_s^4 + Cx_s^2 + D = 0 \tag{20}$$

where the coefficients A, B, C and D are coefficients of α only. Their actual form is rather complex and can be obtained from Gobber and Willamowski [8]. In order to locate the $H3_1$ curve in (r, α) space it is thus necessary for each value of α in $0 < \alpha < 1$ to solve equation (20) for x_s and then substitute this into equations (16) and (17) to find r and then μ.

Codimension-two bifurcations, the most degenerate ones possible in this system, if they occur, will appear on a codimension-one curve in the (r, α) plane. The only one occurring in this system turns out to be one of the $H3_2$ variety, and this occurs on the $H3_1$ curve. These points are located by evaluating the function P_6 of Gobber and Willamowski [8]. One point

of this type occurs in the physical quadrant of parameter space, and a second, on the same branch of the $H3_1$ curve, occurs for negative α and r.

It is worth anticipating the discussion and remarking here that the unfolding of the $H3_2$ point contains phase portraits showing three concentric limit cycles, giving some hope that the inclusion of $\alpha = 0$ in the model might be sufficient to throw light on the computed results discussed in the introduction.

The final part of the analysis involves looking at the possibility of the interaction of static and dynamic bifurcations, i.e. loci where

$$\operatorname{tr} J = 0\,, \qquad \det J = 0 \tag{21}$$

are satisfied simultaneously. Equations (21) imply that the Jacobian matrix has two zero eigenvalues and we refer to this case as the DZE (double zero eigenvalue) bifurcation. Following Gray and Roberts [6] we refer to the simplest of these bifurcations as the saddle-node-Hopf (Sn-H) degeneracy. Using equations (21) along with equations (9) and (10) we can obtain the following explicit form for the Sn-H degeneracy:

$$r = \frac{\alpha^2(1-2\alpha)}{2(1-\alpha)^2}\,, \quad 0 < \alpha < \tfrac{1}{2}\,. \tag{22}$$

It is possible to show that the hysteresis curve is tangential to the Sn-H curve and also that the lower of the two branch $H3_1$ curves meets the Sn-H curve at this point of tangency. One can also show that the $H2_1$ curve and the upper branch of the $H3_1$ curve meet the Sn-H curve at the same point.

Both of these points are examples of more highly degenerate DZE bifurcations (of codimension 2). We are not aware of any rigorous analysis of the unfoldings of these degeneracies along the lines of Guckenheimer and Holmes [9] for the nondegenerate DZE, but they have been unfolded by plausible path-consistency arguments [6].

We cannot obtain further information about the location of the various bifurcation loci in parameter space without numerical integration of the differential equations. Without the qualitative analysis given above and in more detail in [6] such a task would be almost impossible since many of the curves in parameter space lie extremely close together giving regions in parameter space which are sometimes extremely small. This seems to be particularly the case for regions which have the most exotic phase portraits.

3. The quantitative results

The bifurcation loci in the (μ, α) plane differ in a quantitative but important way from the predictions made in [5]. In Fig. 4, for the particular value of $r = 10^{-4}$, we show the saddle-node loci, the loci of $\operatorname{tr} J = 0$ (representing Hopf bifurcation if $\det J > 0$) and the two points on it where $H3_1$ degenerate Hopf bifurcations occur. The intersection of the two saddle-node bifurcation loci is the point of hysteresis bifurcation.

As shown in [6] from each point of intersection of Hopf and saddle-node bifurcation loci there must emanate a homoclinic bifurcation locus and from each $H3_1$ degeneracy there must emanate a locus representing a periodic orbit bifurcation locus (where stable and unstable limit cycles coincide and then disappear). Both these loci are non-local (i.e. they are not

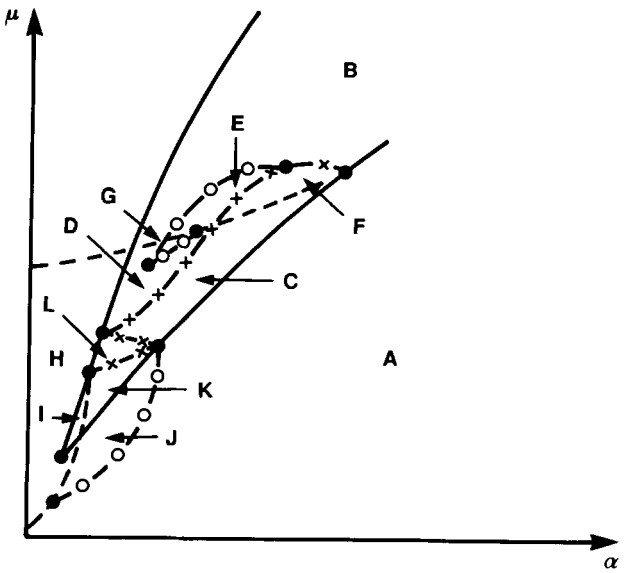

Fig. 4. (α, μ) plot for small r (see [5]).

simply related to the singularities of the system) and can only be obtained by numerical integration of the differential equations.

They are shown in Fig. 5 in detail. The important point for the present paper is that the region G is not in fact entirely contained inside the two saddle-node bifurcation loci as previously assumed [5]. It crosses the upper saddle-node bifurcation locus and creates a new region M in the $\mu - \alpha$ plane in which the phase portrait is simply three concentric limit cycles around an unstable singularity. Not only does this region exist, it also intersects the $\alpha = 0$ axis and persists for small negative (but unphysical) values of α. The width of this

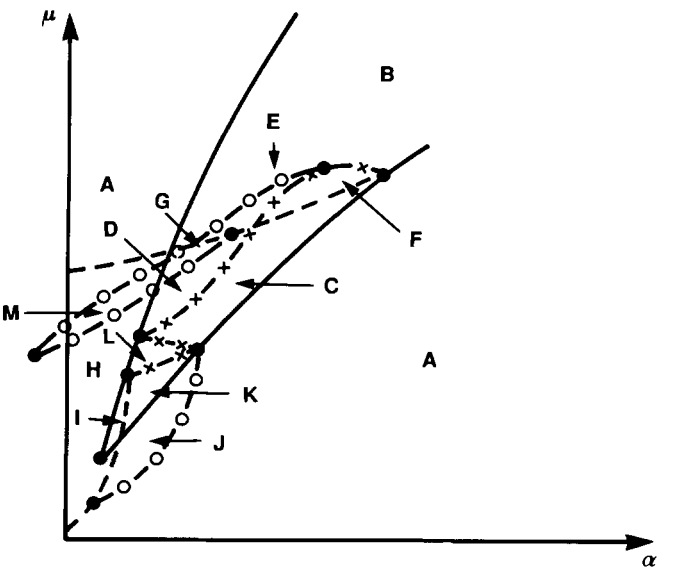

Fig. 5. Modified (α, μ) plot for $r = 10^{-4}$.

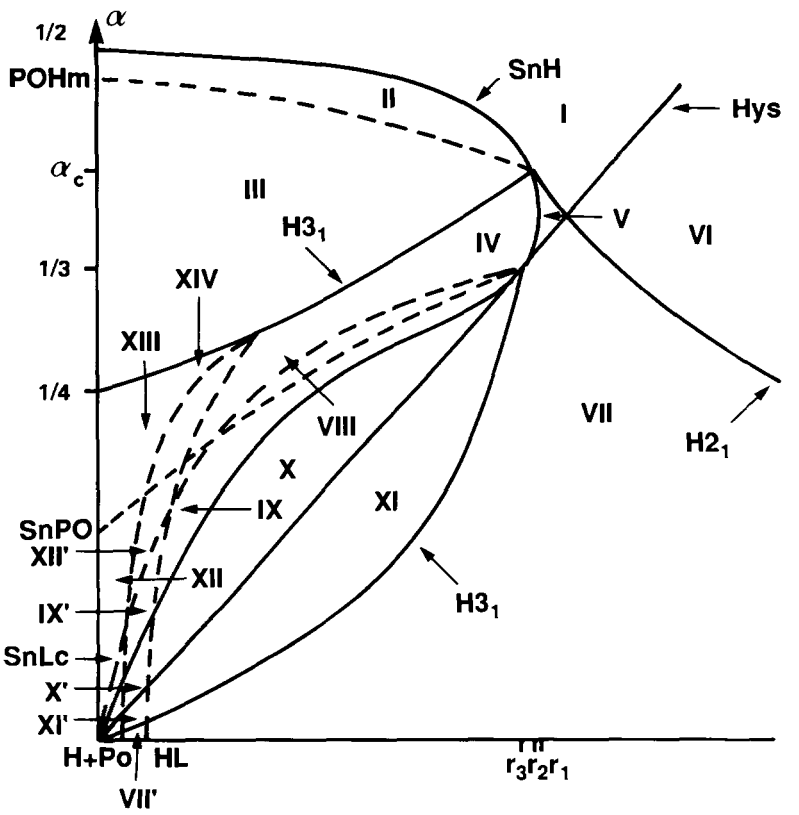

Fig. 6. Modified (r, α) diagram, showing regions of qualitatively distinct bifurcation diagrams.

intersection with the $\alpha = 0$ axis corresponds to the region within which numerical integration of the equations (3) and (4) shows the 'chaotically mixed' oscillations of the earlier figures.

The existence of the intersection of region M with the axis $\alpha = 0$ has repercussions on the behaviour of the system for all values of r. This is shown in Fig. 6 in which the codimension-one (α, r) plot is given. This also differs quantitatively from the plot given in [5] which represents only the *simplest* self-consistent possibility for this system. The numerical work reported here shows that this 'simplest possible' behaviour is not realised, and in fact the actual (α, r) diagram gives rise to five extra bifurcation diagrams compared with the 'simplest possible' behaviour.

These are shown in Fig. 7 along with the most closely related bifurcation diagrams already known to necessarily exist for this system from the 'simplest possible' treatment reported in [5]. In spite of this, only one extra phase portrait (three concentric limit cycles around an unstable singularity) occurs above and beyond the 'simplest possible' case.

4. Conclusions

The cubic autocatalator model for a closed system, represented by the equations

$$dx/dt = \mu - xy^2 - rx\,, \tag{3}$$

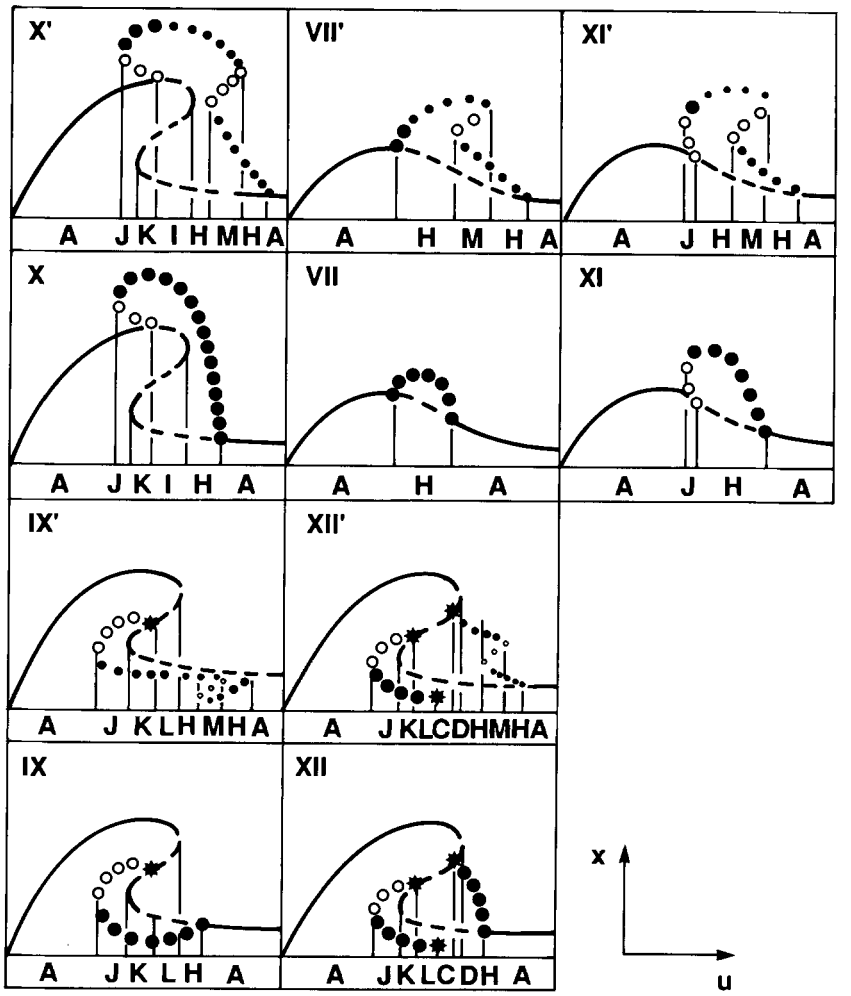

Fig. 7. Additional bifurcation diagrams associated with modifications shown in Fig. 6.

$$dy/dt = xy^2 - y + rx\,, \tag{4}$$

can show two distinct periodic solutions coexisting at the same parameter values in a small but well-defined region of parameter space. This behaviour implies the existence of at least two stable limit cycles and an unstable one, all surrounding the only (unstable) singularity. This behaviour, characteristic of the unfolding of a degenerate Hopf bifurcation of codimension 2, indicates that enlargement of the model to two unfolding parameters would lead to the occurrence of a degenerate singularity of $H3_2$ type.

The unfolding considered here,

$$dx/dt = \mu - xy^2 - rx - \alpha\,, \tag{7}$$

$$dy/dt = xy^2 - y + rx\,, \tag{8}$$

does indeed exhibit a singularity of this type and furthermore the region in parameter space

within which three concentric limit cycles exists does in fact cross the axis $\alpha = 0$. Inside this region apparently chaotically mixed oscillations are exhibited by the computer, confirming our interpretation of these for the original case $\alpha = 0$. For the unfolded model this 'chaotic' behaviour does in fact exist in a region of parameter space with the $H3_2$ singularity on its edge.

The phase portrait in Fig. 3b shows the existence of two limit cycles very close together in a certain region. Numerically this is responsible for the chaotic behaviour that was observed. It is possible, however, that for fixed μ by applying a suitable small perturbation in y whenever x becomes close to zero, one can get either the large or the small limit cycle. Such type of calculations indicate for $\mu > 1.0$, $\alpha = 0$ and for r small $(= 10^{-4})$ that instead of a single stable steady state, we could have a stable steady state surrounded by two limit cycles, one stable and the other unstable which are close together in a certain region. In this case we would not expect mixed oscillations but a large 'excursion' around the stable limit cycle before capture by the attractor. We cannot say whether this behaviour is due to two limit cycles passing very close to the attractor or not.

Acknowledgement

R.A.T. acknowledges the support of the ARGS program grant under the auspices of which this work was carried out.

References

1. P. Gray and S.K. Scott, Autocatalytic reactions in the isothermal continuous stirred tank reactor: isolas and other forms of multistability, *Chem. Eng. Sci.* 39 (1983) 29–43.
2. P. Gray and S.K. Scott, Autocatalytic reactions in the CSTR: oscillations and instabilities in the system $A + 2B \rightarrow 3B$; $B \rightarrow C$, *Chem. Eng. Sci.* 39 (1984) 1087–1097.
3. A. D'Anna, P.G. Lignola and S.K. Scott, The application of singularity theory to isothermal autocatalytic open systems, *Proc. Roy. Soc.* A403 (1986) 341–363.
4. J.H. Merkin, D.J. Needham and S.K. Scott, Oscillatory chemical reactions in closed vessels, *Proc. Roy. Soc.* A406 (1986) 299–323.
5. B.F. Gray, J.H. Merkin and M.J. Roberts, On the structural stability of the cubic autocatalytic scheme in a closed vessel, *Dynamics and Stability of Systems* (in press).
6. B.F. Gray and M.J. Roberts, A method for the complete qualitative analysis of two coupled o.d.e.'s dependent on three parameters, *Proc. Roy. Soc.* A416 (1988) 361–389.
7. J.M.T. Thompson and H.B. Stewart, *Nonlinear dynamics and chaos*, J. Wiley (1986).
8. F. Gobber and K.D. Willamowski, Ljapunov approach to multiple Hopf bifurcation, *J. Math. Anal. Appl.* 71 (1979) 333–350.
9. J. Guckenheimer and P. Holmes, *Nonlinear oscillations, dynamical systems and bifurcations of vector fields*, Appl. Math. Sciences 42, New York, Springer Verlag (1983).